IOP Conf. Series: Materials Science and Engineering **758** (2020) 012064 doi:10.1088/1757-899X/758/1/012064

Evaporation processes of alloying components duringwire-arcdeposition of aluminum alloy 5056

E.S. Salomatova[1], M.F. Kartashev[1], D.N. Trushnikov[1], G.L. Permykov[1], T.V. Olshanskaya[1], I.R. Abashev[1], E.M. Fedoseeva and E.G. Koleva[2]
1 Perm National Research Polytechnic University, Russia
2 Institute of Electronics, Bulgarian Academy of Sciences, Sofia, Bulgaria
E-mail: weld-katy@mail.ru

Abstract. Additive manufacturing technologies are developing fast world wide. Never the less, in the machine-building industry, manufacturing of especially large products is required, and common processes, for example, selective laser melting, are not able to satisfy this requirement. Multilayer wire-arc deposition, allows to make high-quality large-scale products. In addition, the productivity of wire-arc deposition is many times higher than the productivity of powder additive manufacturing. Never the less, the metal obtained by this method is likely to lose easily evaporated alloying elements, which is mainly due to excessive heat and high deposition rates. This process leads to reduced mechanical properties of the deposited metal. The paper presents the results of chemical analysis of the sample obtained by CMT deposition of aluminum alloy 5056.It was revealed that during wire-arc deposition there is evaporation of some alloy components, for example magnesium. A nonlinear theoretical model of nonequilibrium processes in the liquid phase of the deposited metal and the processes of evaporation of chemical easily evaporated elements in the zone of influence of the heating source of wire-arc deposition is presented. Verification of the model was carried out by studying the chemical composition of the samples. During X-ray fluorescence analysis, reduced magnesium content of the first deposited layer was revealed. Increase in the magnesium content was in the upper deposited layers.

1. Introduction

The use of additive technologies helps to reduce the preparatory and technological cycle of creating a product in production, which leads to a reduction in the cost of finished products. Application of wire materials of various compositions expands the range of products obtained in the additive production, in comparison with expensive powder materials. When using wire materials and various surfacing technologies (laser, plasma, CMT surfacing) [1] with technological methods (pneumatic hardening of layers [1-2], ultrasonic action in the process of surfacing), it is possible to obtain products with unique properties, which is an undeniable advantage of additive manufacturing with use of wire materials. This article discusses the samples obtained during CMT (Cold Metal Transfer) surfacing in a pulsed mode. The process of CMT surfacing proceeds as follows: when the deposited wire comes into contact with the surface of the substrate, a short circuit occurs, when the first short circuit is detected, the current decreases to the minimum acceptable value, at the same time, the droplet breaks off due to the reverse movement of the deposited wire. Metal transfer occurs at a current value of almost zero and therefore the contribution of heat is very small [3].

In studies [4] and [5], during investigation of the characteristics of controlling the droplet transfer process with CMT technology it was found that CMT requires less current for the same amount of deposited material as compared to conventional GMAW (Gas Metal Arc Welding).In study [6], the

possibility of using the CMT process for welding of aluminum alloy was investigated. Pires et al. [7] compared the GMAW, the pulsed GMAW and the CMT process and found that the CMT process reduces the emission of harmful fumes due to low heat generation. The above studies provide a preliminary understanding of the CMT process, but the details of the physical processes are still unclear. A complete understanding of the CMT process cannot be obtained by experimental data alone. Thanks to advances in numerical methods and high power computers, the numerical method provides a convenient way to better understand the mechanisms. In recent years, a number of articles have been published on modeling transport phenomena in the process of arc welding [8-11].However, not enough literature is devoted to the CMT-pulsed welding process - a combination of CMT and pulsed arc, especially for welding aluminum alloys and galvanized steel. This technology has been known and used not so long ago, since 2004, so its comprehensive study, including process modeling, is an important and urgent task.

2. Mathematical model

In a first approximation, the mathematical model is based on the solution of the heat problem in a three-dimensional formulation in the first approximation. Due to symmetry, it is sufficient to include only half of the entire object in the computational domain for the description. The geometry of the computational domain is shown in Fig. 1.

The following simplifications were made when modeling the surfacing process. Firstly, the entire volume of the metal under study is in a solid state, secondly, the heating source is written in the form of a Gaussian distribution, thirdly, the geometric parameters of the bead are associated with the parameters of the CMT process.

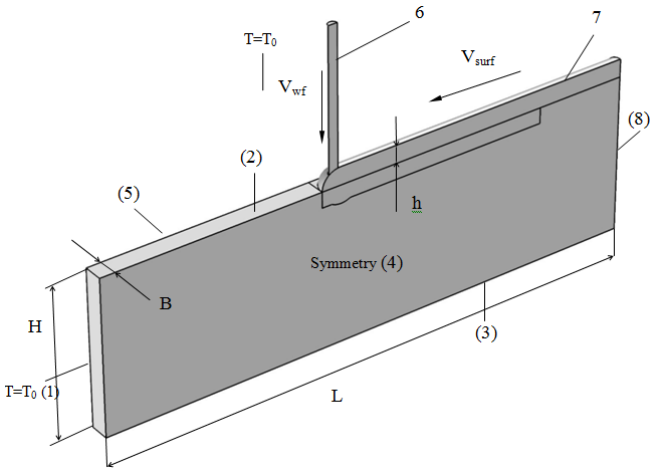

Fig. 1. The design model: 1 – entrance surface; 2 – side surface;3 – bottom surface; 4 – symmetry surface; 5 – top surface; 6 – fused wire; 7 – weld bead; 8 –exit surface

The mathematical model is based on the solution of the differential heat equation (energy transfer) in a three-dimensional formulation

$$— \quad \left(— \quad — \quad —\right) \quad — \quad —— \tag{1}$$

where T is the temperature, $a = \lambda/C_{eff} \cdot \rho$ – coefficient of thermal diffusivity, V – medium velocity (matches surfacing speed and wire feed speed), ρ – density, P – total power input to the product [W/m^3].

The contribution of convective transport in the melt is taken into account by the formula λ_e $\lambda\ (2 - T_L/T)$, where λ_{eff} is the thermal conductivity of a liquid, T_L – liquidus temperature.

The latent heat of fusion and crystallization was taken into account by introducing the effective heat capacity:

$$\frac{p\left[((T \quad _t)/(T \quad))\right]}{\sqrt{(\quad _s)}} \tag{2}$$

whereC_0isheat capacity depending on temperature, H_f– latent heat of fusion, T_{melt} – melting point, which is assumed to be average in the range from solidus temperature T_S to liquidus temperature T_L [12].

In view of symmetry, it is sufficient to include only half of the entire object in the computational domain for description.

Mixed type boundary conditions were used. Thermodynamic boundary conditions on the front surface (surface of the deposited metal):

— —— $(T \quad)$

in the symmetry surface

—

and on all other surfaces

— $(T \quad)$,

where$r = \sqrt{(x - x_0)^2 + (y - y_0)^2}$ is the distance from the axis of the heat source to the considered point (x_0 and y_0 are the coordinates of the center of the source), α_0 – effective heat transfer coefficient taking into account heat loss due to convection and radiation. Table 1 and 2 show the parameters of the surfacing process and the physical characteristics of the deposited material.

Table 1. Parameters of the surfacing process.

Welding current, I (A)	Welding voltage, U (B)	Surfacing speed,V_{surf} (m/s)	Wirefeedspeed, V_{wf} (m /s)	Deposition time of one layer (s)	Pause time between layers (s)
115	17	$1 \cdot 10^{-2}$	$8 \cdot V_{surf}$	16	60

The mass flux density of the i-th alloying element in the wire melting zone is determined by the flux density due to the evaporation of the J_{ev} i-th element, is directly proportional to the impurity concentration

$$\left(S/_S\right), \tag{3}$$

whereJ_0isthe evaporation flux density of the pure i-th element; S_0, S – respectively, the initial and current concentrations of the i-th element in the alloy.

In turn, the density of the diffusion vaporization stream of the i-th element is determined by the formula [13]:

$$\cdot \left(P(T)/\sqrt{\mu \cdot T}\right), \tag{4}$$

whereμ isthe mass in moles of the i-th alloy element; J_v– molar flow of the i-th alloy element; A – dimensional coefficient; $P(T)$ – partial pressure of the i-th component of the melt, which can be determined by the technique described in [14].

Thus, the task is to reduce to a joint solution of equations (1-4) and to determine the mass flow in the volume of the melt carried away from the surface of the melt:

$$\sum_{i=1}^{N}(J_0) \quad — \tag{5}$$

where$\partial m / \partial t$isthemass flow of metal vapor carried away from the surface of the melt.

The initial mass of alloying easily evaporated components in the volume of the molten bath was calculated by the formula

where $V_{melt} \cdot \rho$ is themass of alloy in liquid state, C_i^0 - initial concentration of alloying elements in the weld wire.
The change in the mass of alloying elements during surfacing over time is determined

Thus, we determine the final concentration of alloying elements in the weld bead

The shape of the weld bead was approximated by a semi-ellipse. The volume of deposited per unit time of the bead coincides with the volume of supplied filler material $\pi r_{wire}^2 V_{wf} = \pi a_в b_в V_{pl}/2$, where $a_в$ and $b_в$ are the width and the height of the weld bead, respectively.
Numerical implementation was carried out using the application software package Comsol 4.3 (heat transfer module). The process simulation area was covered with a three-dimensional grid inscribed in the calculation area. The grid had an uneven pitch (Fig. 2). In the zone of arc influence and filler wire feed, the maximum cell size was 0.5 mm, in the rest of the region - 2.5 mm.

During the deposition of aluminum wire, a liquid melt forms in the zone of action of the heating source, as shown in Fig. 3 (b), in this zone the phase transition from the liquid to the solid state is taken into account, as shown in Fig. 3 (a).

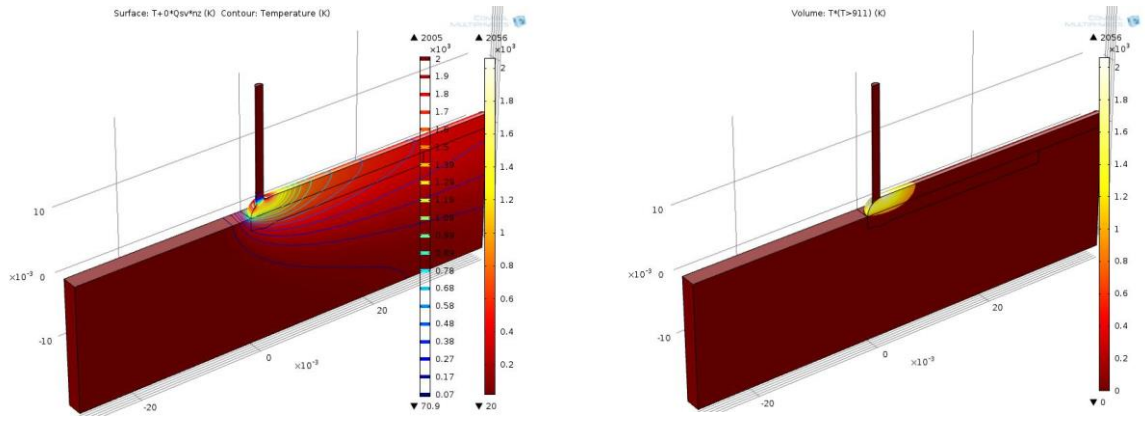

a) b)

Fig. 2. The results of numerical modeling:
(a) zone of metal in liquid and solid states, the maximum temperature of the solid state is 911 K,
(b) action of the heating source, maximum design temperature 2056 K.

With an increase in the power of the heating source during CMT surfacing, we observe a decrease in the concentration of magnesium in the deposited layer.

3. Conclusions

The most probable cause of such a difference in the concentration of magnesium in the deposited layers is the influence of thermal action from each subsequent layer and the high diffusion activity of magnesium. Magnesium in aluminum alloy acts as a hardener. To avoid obtaining deposited products

with reduced strength properties, it is necessary to mechanically remove the first layer deposited on the substrate.

A mathematical model has been developed that describes the processes of evaporation of easily evaporated components of an aluminum alloy, which allows predicting the chemical composition of the beads obtained by CMT surfacing. The mathematical model was verified by conducting a full-scale experiment and comparing the results of chemical analysis of the weld metal zones with the calculated values.

References

[1] Cong B. et al. Influence of cold metal transfer process and its heat input on weld bead geometry and porosity of aluminum-copper alloy welds 2016 *Rare Metal Materials and Engineering* **45** 3 pp 606-611
[2] Shchitsyn Y, Terentyev S, Neubybin S, Artemov A, Belinin D Formation of Structure and Properties of Steel 04CR18NI9 at Additive Production of Trainings 2018 *Vestnik of PNRPU. Engineering, materials science* **20** 3 pp 55-62
[3] Zhang H T, Feng J C, He P, Zhang B, Chen J M, and Wang L The Arc Characteristics and Metal Transfer Behavior of Cold Metal Transfer and its Use in Joining Aluminum to Zinc-Coated Steel 2004 *Mater. Sci. Eng.* **499** pp 111–113
[4] Feng J, Zhang H, and He P The CMT Short-Circuiting Metal Transfer Process and its Use in Thin Aluminum Sheets Welding 2009 *Mater. Des*. **30**
[5] Pickin C G, and Young K, Evaluation of Cold Metal Transfer (CMT) Process for Welding Aluminum Alloy 2006 *Sci. Technol. Weld. Joining* **11** pp 583–585
[6] Pires I, Quintino L, Amaral V, and Rosado T Reduction of Fume and Gas Emissions Using Innovative Gas Metal Arc Welding Variants 2010 *Int. J Adv. Manuf. Technol*. **50**
[7] Rao Z H, Zhou J, Liao S M, and Tsai H L Three-Dimensional Modeling of Transport Phenomena and Their Effect on the Formation of Ripples in Gas Metal Arc Welding 2010 *J. Appl. Phys*. **107** 054905
[8] Rao Z H, Liao S M and Tsai H L Effects of Shielding Gas Compositions on Arc Plasma and Metal Transfer in Gas Metal Arc Welding 2010 *J. Appl. Phys*.**107** 044902
[9] Haidar J Prediction of Metal Droplet Formation in Gas Metal Arc Welding II 1998 *J. Appl. Phys*. **84**, pp 3530–3540
[10] Fan H G and Kovacevic R A Unified Model of Transport Phenomena in Gas Metal Arc Welding Including Electrode, Arc Plasma and Molten Pool 2004 *J. Phys. D: Appl. Phys*. **37** pp 2531–2544
[11] Hu J, and Tsai H L Heat and Mass Transfer in Gas Metal Arc Welding, Part I: The Arc 2007 *Int. J. Heat and Mass Transfer* **50** pp 833–846
[12] Rao Z H, Hu J, Liao S M and Tsai H L Modeling of the Transport Phenomena in GMAW Using Argon–Helium Mixtures. Part I. The Arc 2010 *Int. J. Heat Mass Transfer* **53** pp 5707–5721
[13] Xu G, Hu J and Tsai H L Modeling Three-Dimensional Plasma Arc in Gas Tungsten Arc Welding 2012 *ASME J. Manuf. Sci. Eng*. **134**(3) p 031001
[14] Xu G, Hu J and Tsai H L Three-Dimensional Modeling of Arc Plasma and Metal Transfer in Gas Metal Arc Welding 2009 *Int. J. Heat Mass Transfer* **52** pp 1709–1724

Acknowledgments

This work was financially supported by the Government of the Perm Krai under the agreement S-26/787 of 12/21/2017 and the Russian Foundation for Basic Research in the framework of project No. 18-08-01016 A.